JASMAC
Conference of the Japan Society of Microgravity Application

OR1-1

繊維束状多孔質体内への粘性流体含浸過程とボイド形成に関する数値解析 −複雑流内気液二相流での気液分離制御機構に向けて−

Numerical analysis of viscous fluid impregnation and void formation in a fibrous porous medium —toward a gas–liquid separation control mechanism in complex two-phase flows—

稲川昌樹 [1]，伊藤友起 [1]，上野一郎 [2]
Masaki INAGAWA[1], Tomoki ITO[1], and Ichiro UENO[2]
1　東京理科大学大学院，Tokyo University of Science
2　東京理科大学，Tokyo University of Science

Gas–liquid two-phase flow control is a key challenge in various engineering systems, particularly under microgravity, where capillary effect is dominated [1,2]. An example of such capillarity-dominated two-phase flow can be found in composite manufacturing processes, such as Vacuum Assisted Resin Transfer Moulding (VARTM), where resin impregnation into fibrous porous medium involves displacement of gas by liquid [3]. Accurate prediction of impregnation behaviour and void formation remains difficult, as previous Darcy-scale models cannot capture detailed interface dynamics. This study employs a pore-scale numerical approach to investigate impregnation and macrovoid formation in a single-layer woven fibre bundle. Figure 1 shows the computational domain. A single-layer woven fibre bundle is confined between parallel plates, with fibre volume fraction matched to experimental conditions, resulting in a relatively large modelled fibre diameter. The fluid propaties of liquid and gas are applied to those of 350 cSt silicone oil and air, respectively. Simulations are performed under zero-gravity conditions to replicate microgravity impregnation. The gas–liquid interface is tracked using the Volume of Fluid (VOF) method, with surface tension implemented via the Continuum Surface Force (CSF) model. The capillary number, $\mathrm{Ca} = \mu_\mathrm{l} U_\mathrm{in}/\sigma$, is defined as the ratio of viscous stress to surface tension, where μ_l is the viscosity of liquid, U_in is the characteristic velocity, and σ is the surface tension.

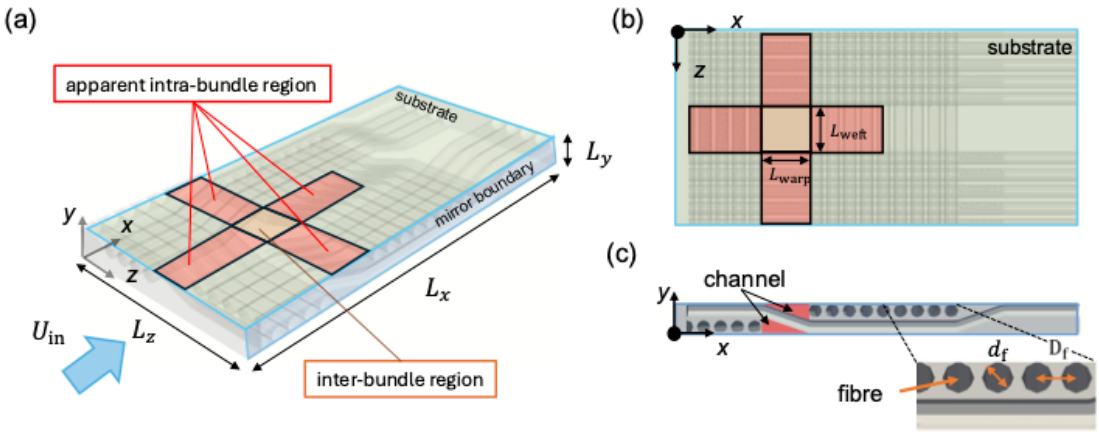

Figure 1. Computional domain: (a) bird-eye view, (b) top view, and (c) side view.

Figure 2 illustrates a representative macrovoid formation sequence. This figure represents how the liquid (shown in deep grey) permeates a single-layer woven fibre bundle (shown in semi-transparent light grey) under $\mathrm{Ca} = 0.001$. For the sake of visibility, the flow fronts near the bottom wall (thin line (in red)) and near the top wall (thick line (in blue)) are also illustrated. The flow front advances nonuniformly along both the top and bottom walls. Intra-bundle regions allow faster liquid penetration, whereas inter-bundle regions exhibit noticeable delays. As a result of this lead–lag behavior across different spatial scales, a first snap-off event occurs in the downstream intra-bundle region adjacent to the top wall (thick blue line, $t^* = 2435$). The trapped gas then persists in the lower part until a second snap-off takes place near the bottom wall (thin red line, $t^* = 2675$), ultimately leading to complete entrapment of the immiscible fluid within the inter-bundle region ($t^* = 2938$). These results provide a detailed description of macrovoid formation through two successive snap-off events, corresponding to mechanical entrapment, and the observed trend agrees with that reported in previous studies [4,5].

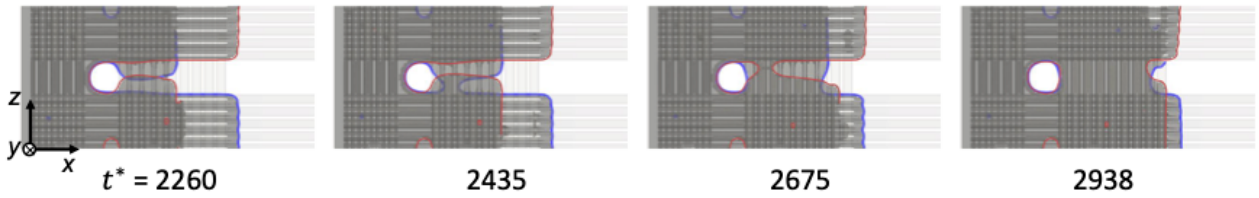

Figure 2. Temporal variation of impregnation of permeating liquid under Ca = 0.001. In each panel, permeating liquid is represented in dark grey, whist fibres and air are represented semi-transparently light grey. Thin- (in red) and thick- (in blue) lines denote flow fronts near bottom wall (at y = 50 μm) and near top wall (at y = 650 μm), respectively.

We analyse the streamwise velocity distribution near the bottom wall under conditions leading to macrovoid formation. Figure 2 shows successive snapshots on a plane at $(x, y = 50\ \mu\mathrm{m}, z)$, with velocity normalized by the inlet velocity. At $t^* = 1525$, high U_x is observed within the intra-bundle region, while the inter-bundle region exhibits much lower U_x, resulting in a non-uniform flow-front advance. As the flow fronts change direction and converge, a snap-off occurs in region (A) at $t^* = 2675$. After this event, the velocity field shows a negative U_x upstream of the upstream-side interface and a positive U_x downstream of the downstream-side interface, indicating the complete entrapment of gas in the inter-bundle region.

These results demonstrate that pore-scale modelling provides valuable insight into capillary-driven impregnation phenomena relevant to both microgravity fluid management and composite manufacturing.

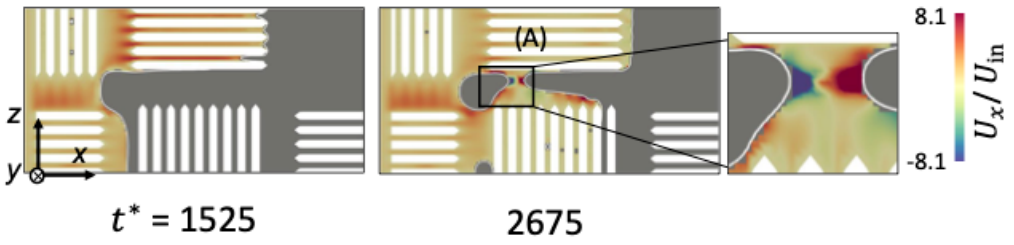

Figure 3. Velocity distribution in streamwise direction before and after snap-off event occurs near flow front near bottom wall (at $y = 50$ μm) under Ca = 0.001.

Acknowledgement

This research was partially supported by the Grant-in-Aid for scientific Research (B) (Grant No.: 24K00824) from the Japan Society for the Promotion of Science (JSPS). One of the authors, MI, acknowledges the Advanced Centre for Computational Materials Science (ACCMS), Kyoto University, for providing their supercomputer resources (JFY2024 & 2025) for the part of the present simulations.

References

1) P. Eckart, Spaceflight Life Support and Biospherics, Vol. 5, *Springer Science & Business Media*, 2013.
2) S.P. Eshima and J.A. Nabity, Impact of dormancy on ECLSS design and operation: A review, *Acta Astronautica*, 223 (2024) 304–315.
3) H. Teixidó, et al., Capillary effects in fiber reinforced polymer composite processing: A review, *Frontiers in Materials*, 9 (2022) 809226.
4) K. Yoshihara, et al., Effect of wettability on viscous fluid impregnation in single-layer woven-fibre bundles driven by pressure difference, *Composites Part A: Applied Science and Manufacturing*, 138 (2020) 106049.
5) C. Devalve and R. Pitchmani, Simulation of void formation in liquid composite molding processes, *Composites Part A: Applied Science and Manufacturing*, **51** (2013) 22-32